A Terminology

In Table A1, we present an overview of the different states and the terminology used throughout the manuscript.

Table A1: Notations related to the compartments in the model

State	Description
$\boldsymbol{S}(t)$	Susceptible individuals
$\boldsymbol{E}(t)$	Infected individuals not being infectious yet
$\boldsymbol{I_{presym}}(t)$	Individuals pre-symptomatically infected
$\boldsymbol{I_{asym}}(t)$	Asymptomatically infected individuals
$\boldsymbol{I_{mild}}(t)$	Infected individuals with mild symptoms
$\boldsymbol{I_{sev}}(t)$	Infected individuals with severe symptoms requiring hospitalization
$\boldsymbol{I_{hosp}}(t)$	Hospitalized individuals
$\boldsymbol{I_{icu}}(t)$	Individuals admitted to intensive care unit
$\boldsymbol{D}(t)$	Number of deaths
$\boldsymbol{R}(t)$	Recovered individuals

B Model parameters

In this appendix, we provide a detailed overview of the different assumptions related to the transmission process and the change in behaviour upon (severe) symptomatic infection.

B.1 Susceptibility and infectiousness in children

Until recently, there was no (conclusive) evidence of differential infectiousness and/or susceptibility to COVID-19 infection in children. Some authors claimed that no significant differences in viral load were present between (symptomatic) children and adults, even after revising their work [1]. A re-analysis of these (initial) findings by Held and McConway and Spiegelhalter [2, 3], however, clearly shows that children between 1 and 10 years old have on average only 27% (95% CI: 8% - 91%) of the viral load of adults aged 20 years or more. For the mathematical model proposed here, we do not differentiate between infectiousness and susceptibility in children as compared to adults directly [4]. However, as children are presumed to be more likely to have a higher probability of being asymptomatically infected (see Section B.2), and the relative infectiousness of asymptomatic versus symptomatic individuals r_β is (assumed) equal to 0.51 [5], children are implicitly less infectious, hence, contribute less to the transmission process relative to adults.

B.2 Age-dependent proportions of asymptomatic cases

The age-dependent proportions of asymptomatic cases, represented by the vector $\boldsymbol{p}$, are based on a study by Wu et al. (2020) [6]. More specifically, we use the age-specific relative susceptibility to symptomatic infection reported by Wu et al. (2020) [6] to inform the proportion of asymptomatic cases. In order to do so, we start from an overall age-weighted proportion of asymptomatic cases in the Belgian population equal to 50% [6] implying that

$$\boldsymbol{p} = (0.94, 0.90, 0.84, 0.61, 0.49, 0.21, 0.02, 0.02, 0.02, 0.02)^T.$$

Although we are fixing the age-dependent proportions of asymptomatic cases in the model, we do

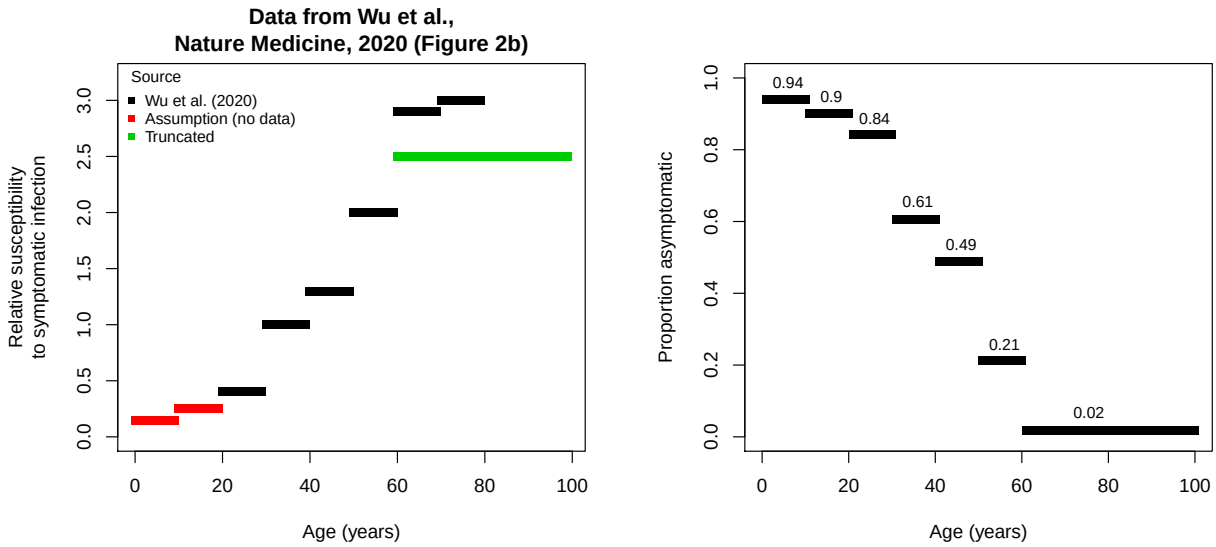

Figure B12: Relative susceptibility to symptomatic infection as a function of age (in years) reported by Wu et al. (2020) [6] (left panel) and the proportion of asymptomatic cases by age relying on the assumption of 50% of asymptomatic infections.

allow for differential probabilities of hospitalization through the specification of an age-dependent probability of only having mild symptoms upon being symptomatic. The reason for this constraint is the fact that based on the available data, we cannot disentangle the age-specific probability of being asymptomatic from the probability of having mild symptoms.

B.3 Symptom severity upon symptomatic infection

In Table B1, the proportion of hospitalizations and ICU admissions are reported for COVID-19 cases by age group in the United States (between February 12 - March 16, 2020) [7].

Table B1: Hospitalization and Intensive Care Unit (ICU) admission percentages (%) for reported COVID-19 cases by age group based on data from the USA, February 12 - March 16, 2020 [7].

Age group	Hospitalization	Average	ICU	Average	Age group	ϕ_0	ϕ_1
0-19	1.6-2.5	2.05	0.0	0.00	[0,10)	98.0	100.0
20-44	14.3-20.8	17.55	2.0-4.2	3.10	[10,20)	98.0	100.0
45-54	21.2-28.3	24.75	5.4-10.4	7.90	[20,30)	79.0	85.0
55-64	20.5-30.1	25.30	4.7-11.2	7.95	[30,40)	79.0	85.0
65-74	28.6-43.5	36.05	8.1-18.8	13.45	[40,50)	67.0	76.0
75-84	30.5-58.7	44.60	10.5-30.0	20.25	[50,60)	67.0	76.0
≥ 85	31.3-70.3	50.80	6.3-29.0	17.65	[60,70)	50.0	73.0
					[70,80)	35.0	69.0
Total	20.7-31.4	26.05	4.9-11.5	8.20	[80,100)	32.0	74.0

In our model, we estimate the age-specific probability of developing only mild symptoms $\boldsymbol{\phi}_0$. Furthermore, the probabilities $\boldsymbol{\phi}_1$ are fixed to the values reported in Table B1. Note that if, for example, $\phi_1(k) = 0.75$ and $\phi_0(k) = 0.8$, representing the probability of hospitalization conditional on having severe symptoms and the probability of having mild symptoms in age group k, then the probability of hospitalization in symptomatic individuals is equal to $0.2 \times 0.75 = 0.15$. Since we lack detailed

age-specific information about the relative proportions of ICU admissions as compared to the total number of hospitalizations, and data on referral between ICU and hospital wards throughout hospital stay, we are not able to inform ϕ_1.

B.4 Case fatality rates - Probability of dying upon hospitalization

Age-dependent case fatality rates have been adopted from Riou et al. (2020) [8] which were estimated from outbreak data obtained in Hubei, China in the period January to February. In Table B2, we present these age-specific case-fatality rates $\tilde{\mu}(k)$ (number of deaths relative to confirmed cases). In our analysis, the rates $\mu(k)$ are rather representing the probability of dying upon hospitalization (deaths relative to number of hospitalized individuals), taken to be equal for hospitalized individuals and critically ill individuals (i.e., $\mu(k) \equiv \mu_{hosp}(k) = \mu_{icu}(k)$), which also relates to the inability of disentangling hospitalization from ICU admission based on the available data. In the stochastic model, however, we estimate these rates $\mu(k)$ from the available mortality data. Due to the low number of deaths in young age categories, we assume that $\mu(1) = 0$ and $\mu(2) = \mu(3)$, comprising parameters to be estimated from the data. A complete list of model parameters with reference values is presented in Table B3.

Table B2: Age-dependent case-fatality rates.

[0-10)	[10-20)	[20-30)	[30-40)	[40-50)	[50-60)	[60-70)	[70-80)	[80-90)	[90, ∞)
0.000094	0.00022	0.00091	0.0018	0.004	0.013	0.046	0.098	0.18	0.18

B.5 Overview of epidemiological and model parameters

An overview of important epidemiological parameters related to SARS-CoV-2/COVID-19 transmission dynamics is provided in Table B3 together with relevant sources. Some of these parameters are directly or indirectly included in the modeling approach. In the last column we indicate whether these parameters are estimated or fixed in the estimation procedure. A detailed overview of all model parameters can be found in the next subsection.

B.6 Prior distributions

In Table B4, we present an overview of the prior distributions considered for the various model parameters.

Table B3: List of epidemiological parameters; *: for asymptomatic individuals only.

Notation	Description	Value	Source	Model
ρ^{-1}	Average length of incubation period	5.2 (4.1, 7.0) 5.2 days 5 days 4 days	[5] [9] [10] [11]	Estimated
γ^{-1}	Average length of latency period	2 days	–	Estimated
θ^{-1}	Average length of pre-symptomatic infectious period	3.2 days	$\rho^{-1} - \gamma^{-1}$	Estimated
σ^{-1}	Average length of infectious period	4.5 days 5 days* 6 days* 5–7 days 9.3 (7.8, 10.0)	[12] [13] [14] [4, 15] [16]	–
$\omega^{-1} + \delta_2^{*-1}$	Average time between (severe) symptom onset and hospitalization	5.9 (0.8, 11.0) 2.7 (1.6, 4.1) 3 – 10.4	[17] [10] [18]	Estimated
δ_1^{-1}	Average length of infectious period when asymptotically infected (after pre-symptomatic phase)	3.5 days	–	Estimated
δ_2^{*-1}	Average length of infectious period when mildly infected (after pre-symptomatic phase)	3.5 days	–	Estimated
δ_3^{*-1}	Recovery period of hospitalized individuals – length of stay in the hospital	11.5 (8.0, 17.3) 13.3 (7.3, 19.3)	[19] [17]	Estimated
δ_4^{*-1}	Recovery period of critically infected in ICU – length of stay in ICU	14 days	–	Estimated
p	Proportion of asymptomatic cases	0.42 (0.17, 0.67) 0.35 (0.30, 0.39)	[20, 21] [22]	Fixed
$1 - \phi_0$	Proportion of symptomatic cases developing severe to very severe symptoms	0 (children) 0.1 (adults) 0.2 (seniors) 0.2 (constant)	[23] [24] [25] –	Estimated
ϕ_0	Proportion of symptomatic cases developing only mild symptoms	$1 - (1 - \phi_0)$	–	Estimated
$1 - \phi_1$	Proportion of hospitalized persons requiring ICU admission	0.25 (constant)	–	Fixed
r_β	Relative infectiousness of pre-symptomatic and asymptomatic individuals	0.51	[5]	Fixed
R_0	Basic reproduction number	2.24 (1.96, 2.25) 2.35 (1.15, 4.77) 2.36, 2.5 3.00 (2.80, 3.20) 3.00 (2.60, 3.30) 3.10 (2.90, 3.20) 3.60 (3.49, 3.84) 3.60 (3.20, 4.20	[26] [27] [28, 29] [30] [31] [32] [33] [34]	Estimated

Table B4: Prior distributions for the model parameters.

	Baseline scenario	
Parameter	Prior distribution	# parameters
γ	$N(0.500, 0.050^2)$	1
θ	$N(0.286, 0.050^2)$	1
δ_1	$N(0.286, 0.050^2)$	1
δ_2^*	$\mathrm{Un}(0,1)$	1
δ_3^*	$\mathrm{Un}(0,1)$	1
$\omega(k)$	$\mathrm{Un}(0,1)$	10
β_1^*	$\mathrm{Un}(0,5)$	1
$\phi_0(k)$	$\mathrm{Un}(0,1)$	10
$\mu(k)$	$\mathrm{Un}(0,1)$	8
R_0	$N(2.500, 0.100^2)$	1

C Social contact data

C.1 Baseline contact matrices

The contact matrices for the asymptomatic individuals ($\boldsymbol{C}_{asym}$) is taken to be equal to the general contact matrices collected in the Belgian survey in 2010–2011. Thus we assume that individuals do not change their contact behaviour when being asymptomatically infected with COVID-19. The overall contact matrix is the sum of the contact matrices encompassing contacts made at the following locations: home, work, school, transportation, leisure and other places.

Thus $\boldsymbol{C}_{asym}$ is obtained as follows:

$$\boldsymbol{C}_{asym} = \boldsymbol{C}_{home} + \boldsymbol{C}_{work} + \boldsymbol{C}_{school} + \boldsymbol{C}_{leisure} + \boldsymbol{C}_{transport} + \boldsymbol{C}_{other}$$

In Figure C1, we graphically depict the social contact matrix $\boldsymbol{C}_{asym}$ in terms of the average number of daily contacts for individuals of different age groups contacting each other. The contact matrices for symptomatic individuals are obtained by re-scaling the matrix $\boldsymbol{C}_{asym}$ in the respective locations by the relative change in the number of contacts observed by Van Kerckhove et al. [35] during the 2009 A/H1N1 pandemic Influenza in England. Hence, we presume that social contacts are adapted in a similar way in the Belgian population upon contracting the disease and experiencing symptoms. Thus, $\boldsymbol{C}_{sym}$ is defined as a weighted sum of the aforementioned contact matrices at specific locations, i.e.,

$$\boldsymbol{C}_{sym} = \boldsymbol{C}_{home} + 0.09\boldsymbol{C}_{work} + 0.09\boldsymbol{C}_{school} + 0.13\boldsymbol{C}_{transport} + 0.06\boldsymbol{C}_{leisure} + 0.25\boldsymbol{C}_{other}$$

C.2 Intervention contact matrices

The contact matrices for the asymptomatic individuals during the lockdown depend on the intervention considered (see Table 1). The contact matrices made in all locations are changed except for the one accommodating contacts made at home. The framework of assigning relative reductions to the social contact matrices obtained at the different locations can be illustrated as follows:

$$\boldsymbol{C}_{asym} = \boldsymbol{C}_{home} + \alpha\boldsymbol{C}_{work} + \alpha\boldsymbol{C}_{transport} + \beta\boldsymbol{C}_{school} + \rho\boldsymbol{C}_{leisure} + \rho\boldsymbol{C}_{other},$$

where $1-\alpha$ represents the percentage of telework considered (people working from home and/or who have stopped working), β represents the percentage of school contacts retained (hence, 0 in

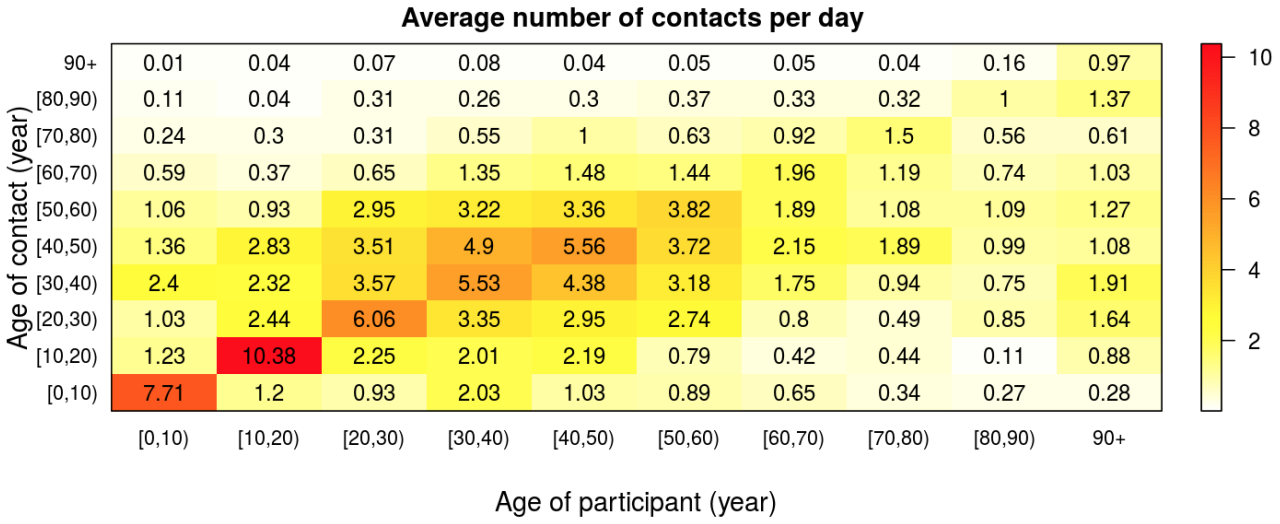

Figure C1: Average number of contacts per day between individuals of different age classes - social contact matrix $\boldsymbol{C_{asym}}$ based on the social contact data from Belgium anno 2010–2011.

case of school closure), ρ represents the fraction of contacts during leisure and other activities that are still made given the imposed measures targeting physical distancing. The contact matrices of the symptomatic $\boldsymbol{C}_{sym}$ are obtained in a similar manner:

$$\boldsymbol{C}_{sym} = \boldsymbol{C}_{home} + \alpha\left(0.09\boldsymbol{C}_{work} + 0.13\boldsymbol{C}_{transport}\right) + 0.09\beta\boldsymbol{C}_{school} + \rho\left(0.06\boldsymbol{C}_{leisure} + 0.25\boldsymbol{C}_{other}\right).$$

All location-specific contact matrices from the Belgian social contact survey in 2010 are directly

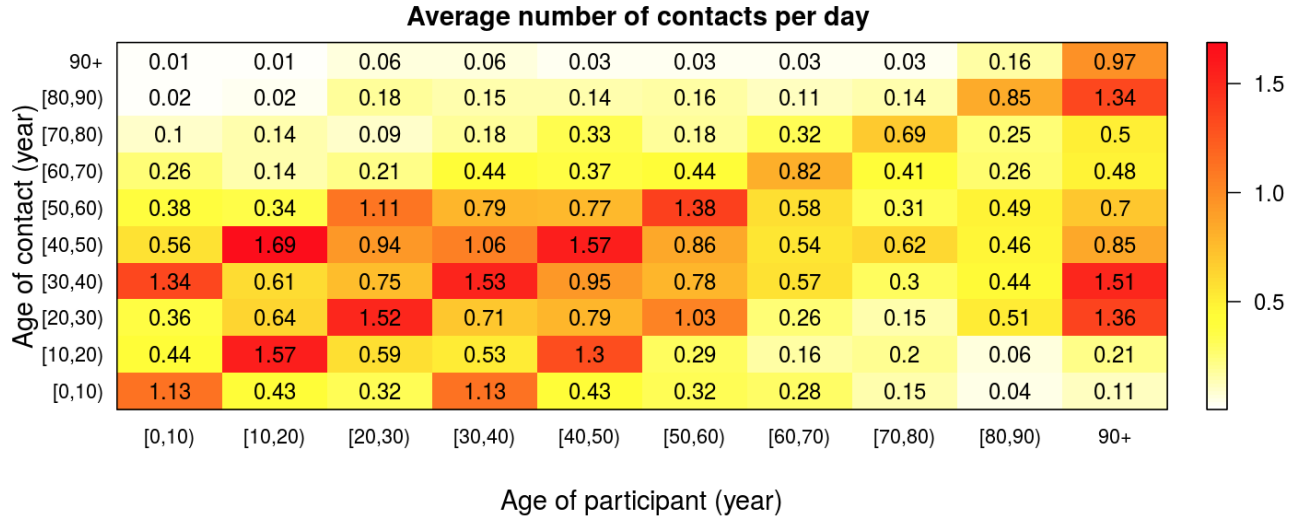

Figure C2: Average number of contacts per day between individuals of different age classes - social contact matrix $\boldsymbol{C_{asym}}$ based on the social contact data from Belgium anno 2010–2011 after intervention measures are imposed according to the 80% TW & SC scenario outlined in Table 1.

available at http://www.socialcontactdata.org/socrates/.

The performance of the matrices presented in Table 1 are compared based on the Deviance Information Criterion (DIC), introduced by Spiegelhalter et al. [36] to compare the relative fit of a set of

Bayesian hierarchical models. DIC is a relative measure balancing goodness-of-fit and complexity of a model and is based on the deviance. An overview of the respective DIC-values related to the different choices of the intervention contact matrices is presented in Table C5.

Table C5: Deviance Information Criterion (DIC) values for the different social contact matrices considered to quantify the impact of the intervention measures on social contact patterns. Percentage of average number of pre-pandemic contacts at different locations. WT: Work and transport reductions, SC: School closure.

Social contact matrix	Work & Transport	School closure	Leisure & other activities	DIC
50% WT & SC	50%	Yes	10%	12930.98
60% WT & SC	40%	Yes	10%	12896.75
70% WT & SC	30%	Yes	10%	12459.82
80% WT & SC	20%	Yes	10%	11577.97
90% WT & SC	10%	Yes	10%	12477.25

D Hospitalization incidence data

In Figure D1, we depict the weekly age distribution of hospitalized cases derived from the clinical surveillance database of COVID-19 hospitalized patients during the first wave of COVID-19 in Belgium. As mentioned in the main text, the day of introduction is considered to be March 1, 2020.

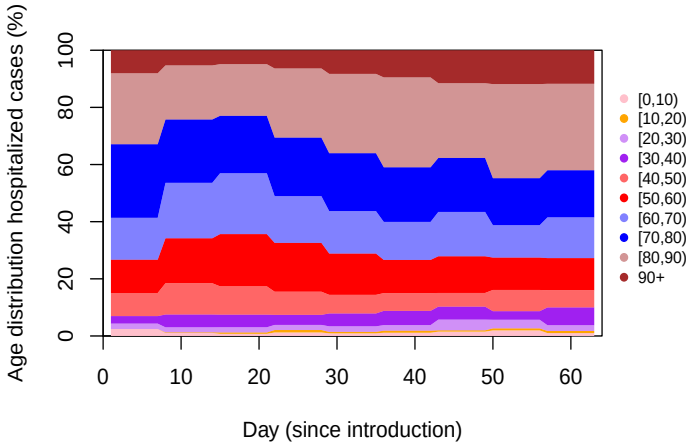

Figure D1: Weekly age distribution of hospitalized patients in Belgian hospitals during the first COVID-19 wave in Belgium.

E Serological survey data

We use serial serological survey data collected during two cross-sectional periods and based on residual samples coming from 10 private laboratories [37]. Serological survey data is collected at different cross-sectional sampling times and blood samples are tested for the presence of IgG antibodies against the SARS-CoV-2 virus. Consequently, individuals are classified as seronegative,

equivocal or seropositive based on their measured IgG antibody concentration against S1 proteins of SARS-CoV-2 obtained from the EuroImmun semi-quantitative ELISA test kit (EuroImmun, Luebeck, Germany). The age-specific seroprevalence is derived as the proportion of seropositive individuals in each age class.

In order to relate the model-based prevalence of COVID-19 in the population to the observed seroprevalence, we assume that the seroprevalence at calendar time t and age a is denoted by $\pi(a,t)$ and that IgG antibodies against SARS-CoV-2 are detectable upon infection according to the following logistic function:

$$p_{sens}(t_0) = \text{expit}(\beta_0 + \beta_1 t_0) = \frac{\exp(\beta_0 + \beta_1 t_0)}{1 + \exp(\beta_0 + \beta_1 t_0)},$$

where $p_{sens}(t_0)$ represents the probability of having a sufficiently high IgG antibody concentration to indicate past SARS-CoV-2 infection. The sensitivity of the diagnostic tests is considered to be a function of the time since symptom onset t_0 (at least in the presence of symptoms), i.e. sensitivity of the diagnostic testing procedure as a function of time since onset of symptoms presuming a sensitivity of zero prior to symptom onset. In this modeling approach, we rely on estimates of the sensitivity curve obtained from the literature [38], reaching a sensitivity of 99% 14 days after symptom onset, albeit that sufficient information regarding the sensitivity of the specific diagnostic test in use is currently lacking. In this exercise, specificity of the test is presumed to be very high (100%), implying no false positive test results. A lower specificity would lead to more false positive cases, thereby overestimating the seroprevalence as compared to the true underlying prevalence in the population. Since the model is calibrated on hospitalization data, the increase in false positives would imply an underestimation of the probability of hospitalization and an overestimation of the total number of infected cases in the population (the so-called dark number). However, we do believe that the general conclusions with regard to the impact of exit strategies on the burden of the healthcare system through the number of hospitalizations and deaths are not affected by this lower specificity, especially since there is little acquired immunity.

The total number of individuals of age a at the time of data collection t (expressed as days since the start of the epidemic) in the population that will test positive can be written as:

$$n_p(a,t) = \sum_{j=0}^{t} p_{sens}(j) \left\{ I^{new}_{sym,t-j}(a) + I^{new}_{asym,t-j}(a) \right\},$$

where $I^{new}_{sym,t}(a)$ and $I^{new}_{asym,t}(a)$ refer to the number of new individuals of age a with symptom onset at time t and the number of individuals of age a entering the asymptomatic state at time t, respectively. Although still uncertain to date, asymptomatic individuals are presumed to be similar to symptomatic ones in terms of their humoral immune response following exposure to the SARS-CoV-2 virus.

More recently, Borremans et al. (2020) [39] showed that IgG antibody detection probabilities increase with time since symptom onset, implying that nearly all (98–100% of) individuals had detectable antibodies by day 22–23 after symptom onset. Although detection probabilities are estimated based on different assays, these authors showed that all assays exhibit comparable growth rates except for a slower increase in antibody levels for IgG ELISA-Spike assays. As a sensitivity analysis, we show the impact of altering the logistic sensitivity curve $p_{sens}(t_0)$ (black line) with a delayed 99% detectability of IgG antibodies in line with the aforementioned findings by Borremans et al. (2020) (red line in Figure E2) in Appendix F.

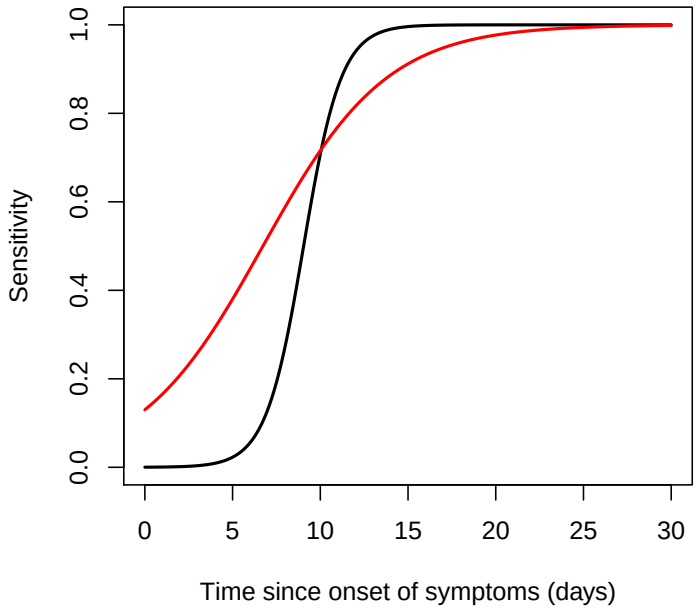

Figure E2: Presumed sensitivity curves with time since onset of symptoms. The black solid line represents the sensitivity curve constructed based on results in Lou et al. (2020) [38] and the red line is based on the findings by Borremans et al. (2020) [39].

F Additional results

F.1 Posterior summary measures

Here, we present an overview of the posterior mean, median and 95% credible intervals (CIs) for all model parameters, and parameters derived thereof, in the final model (Table F1). In total, the final model has 35 parameters. As mentioned in Appendix B, the vectors defining the age-specific probability of being asymptomatic $\boldsymbol{p}$ and the probability of regular hospitalization versus ICU admission $\boldsymbol{\phi}_1$ are fixed, $\boldsymbol{\delta}_2 = \boldsymbol{\phi}_0\delta_2^*$ and $\boldsymbol{\psi} = (1-\boldsymbol{\phi}_0)\delta_2^*$. Moreover, $\boldsymbol{\delta}_3 = \boldsymbol{\delta}_4 = (1-\boldsymbol{\mu})\delta_3^*$ and $\boldsymbol{\tau}_1 = \boldsymbol{\tau}_2 = \boldsymbol{\mu}\delta_3^*$. Note that $\mu(1)$ is fixed to zero as there are no deaths observed in the age group $[0, 10)$ and $\mu(2) = \mu(3)$ given the very small number of deaths in age groups $[10, 20)$ and $[20, 30)$. Furthermore, q is an implicit model parameter governing the extent of R_0. Prior distributions for all 35 model parameters are listed in Table B4.

F.2 Number of individuals in different compartments

In Figure F1, the evolution of the proportions of susceptible, exposed, pre-symptomatic, asymptomatic, mildly infected and individuals with severe symptoms (prior to hospitalization) are shown by age group until May 4, 2020.

F.3 Compliance to intervention measures

The compliance to the intervention measures is modelled using a logistic curve which is depicted in Figure F2. Full compliance to the measures is reached after approximately 6 days.

Table F1: Posterior mean, median and 95% credible interval for the model parameters; CI: credible interval.

Parameter	Mean	Median	95% CI	Parameter	Mean	Median	95% CI
q	0.051	0.051	(0.049, 0.54)	δ_1	0.240	0.240	(0.224, 0.262)
γ	0.729	0.730	(0.672, 0.791)	δ_2^*	0.756	0.756	(0.713, 0.806)
θ	0.475	0.476	(0.434, 0.523)	δ_3^*	0.185	0.185	(0.171, 0.200)
β_1^*	1.404	1.401	(1.283, 1.551)	R_0	2.900	2.899	(2.885, 2.918)
$\phi_0(1)$	0.972	0.972	(0.968, 0.975)	$\phi_0(6)$	0.971	0.971	(0.969, 0.972)
$\phi_0(2)$	0.992	0.992	(0.991, 0.993)	$\phi_0(7)$	0.958	0.958	(0.956, 0.960)
$\phi_0(3)$	0.984	0.984	(0.982, 0.985)	$\phi_0(8)$	0.926	0.926	(0.922, 0.929)
$\phi_0(4)$	0.987	0.987	(0.986, 0.988)	$\phi_0(9)$	0.956	0.956	(0.954, 0.958)
$\phi_0(5)$	0.977	0.977	(0.975, 0.978)	$\phi_0(10)$	0.926	0.926	(0.921, 0.930)
$\omega(1)$	0.167	0.142	(0.102, 0.335)	$\omega(6)$	0.275	0.275	(0.244, 0.306)
$\omega(2)$	0.095	0.094	(0.061, 0.139)	$\omega(7)$	0.343	0.342	(0.315, 0.371)
$\omega(3)$	0.099	0.099	(0.080, 0.120)	$\omega(8)$	0.378	0.374	(0.342, 0.431)
$\omega(4)$	0.162	0.161	(0.142, 0.187)	$\omega(9)$	0.334	0.335	(0.308, 0.361)
$\omega(5)$	0.338	0.338	(0.306, 0.370)	$\omega(10)$	0.302	0.304	(0.252, 0.336)
$\mu(1)$	–	–	–	$\mu(6)$	0.068	0.068	(0.060, 0.076)
$\mu(2)$	0.005	0.005	(0.001, 0.011)	$\mu(7)$	0.183	0.184	(0.170, 0.195)
$\mu(3)$	0.005	0.005	(0.001, 0.011)	$\mu(8)$	0.325	0.325	(0.310, 0.340)
$\mu(4)$	0.024	0.024	(0.017, 0.033)	$\mu(9)$	0.446	0.446	(0.430, 0.464)
$\mu(5)$	0.037	0.037	(0.030, 0.045)	$\mu(10)$	0.611	0.611	(0.568, 0.653)

F.4 Time-dependent reproduction number

In Figure F3, we display the effective reproduction number over time with a 95% credible interval as a red shaded area around the posterior mean. The reproduction number decreased from 2.900 prior to the lockdown to a value of 0.738 (95% CI: 0.732, 0.744) on May 4, 2020.

F.5 Mortality rates

Age-specific mortality rates are presented in Figure F4. Mortality rates are considered to be equal for persons admitted to ICU and to a regular hospital ward as no distinction could be made between referrals within hospitals, nor between deaths in ICU and hospital wards. Needless to say, mortality rates increase by age with the highest mortality rate in the 90+ age category.

F.6 Infection fatality rates

Infection fatality rates (IFRs) are calculated based on the observed number of deaths by age group and the estimated total number of infections in a specific age group (thereby accounting for asymptomatic infections) by May 4, 2020. The overall IFR is estimated to be equal to 0.507% (95% credible interval: 0.480%, 0.536%), excluding nursing home deaths. Note that the model disregards the number of deaths in elderly homes (as this is considered to be a separate COVID-19 outbreak which is not fully accommodated in the considered approach), thereby potentially underestimating the IFRs in the highest age groups, at least if the increase in deaths exceeds the increase in additional infections in nursing homes. Next to that, individuals infected prior to May 4, 2020 that will pass away after that date are not included in the calculations, thereby underestimating the IFRs. A more thorough estimation of the IFRs is performed by Molenberghs et al. (2020) [40],

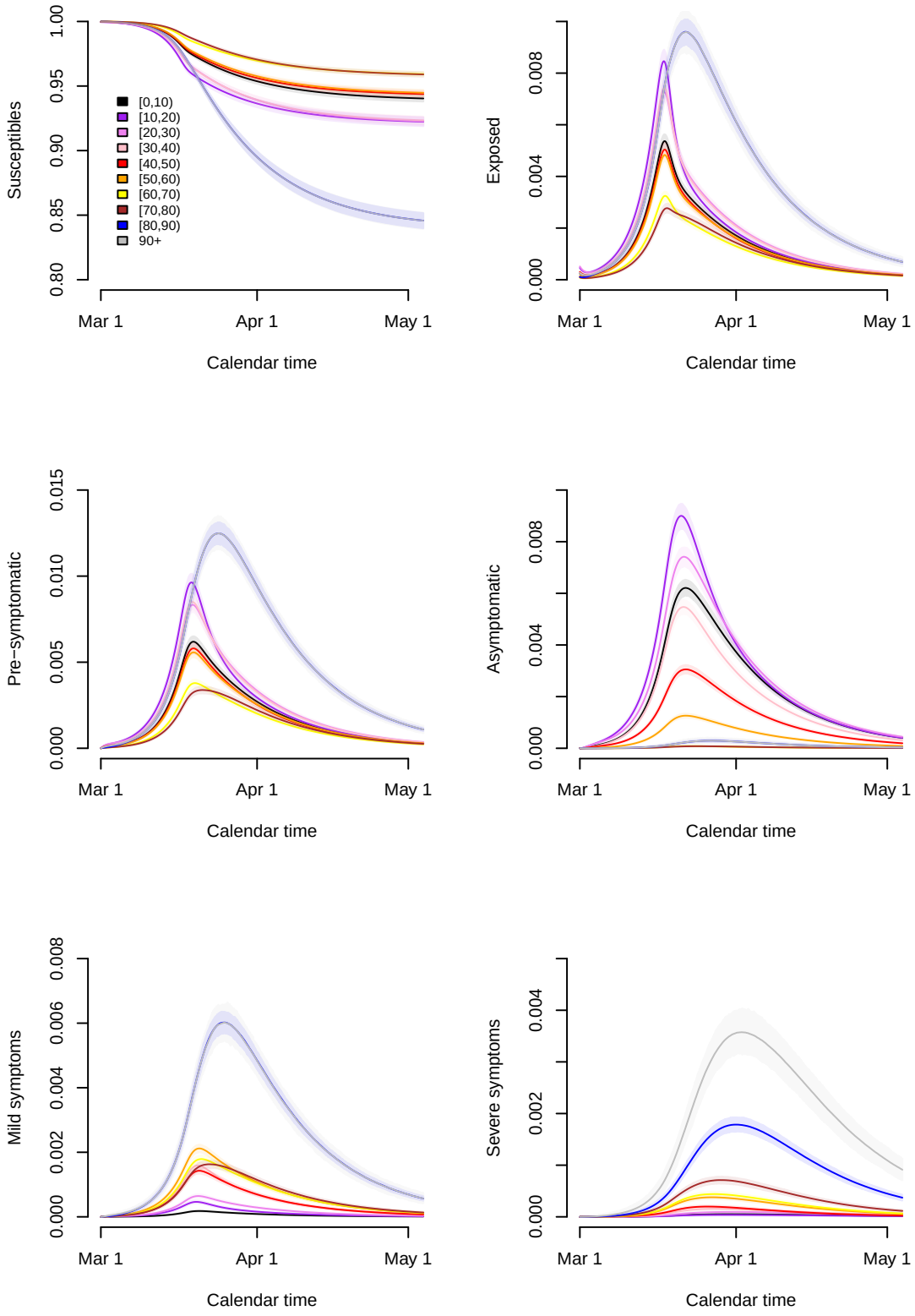

Figure F1: Evolution of the proportion of individuals in the different compartments by age group.

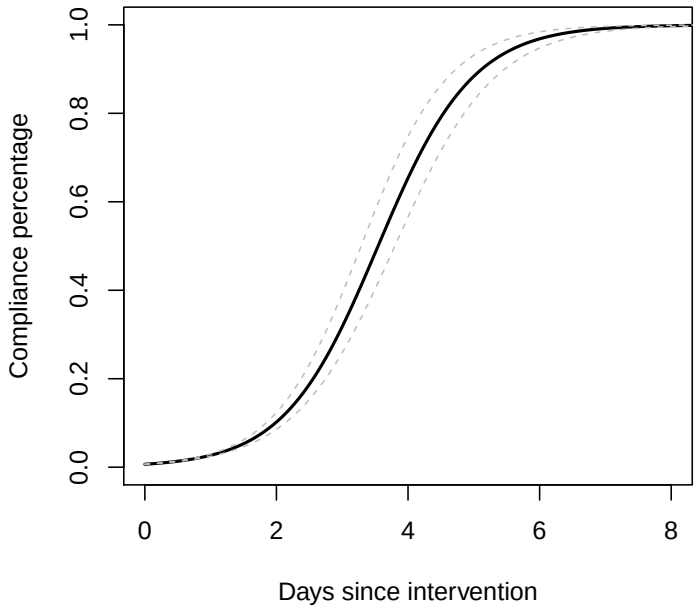

Figure F2: Estimated compliance function to the intervention measures taken by the government.

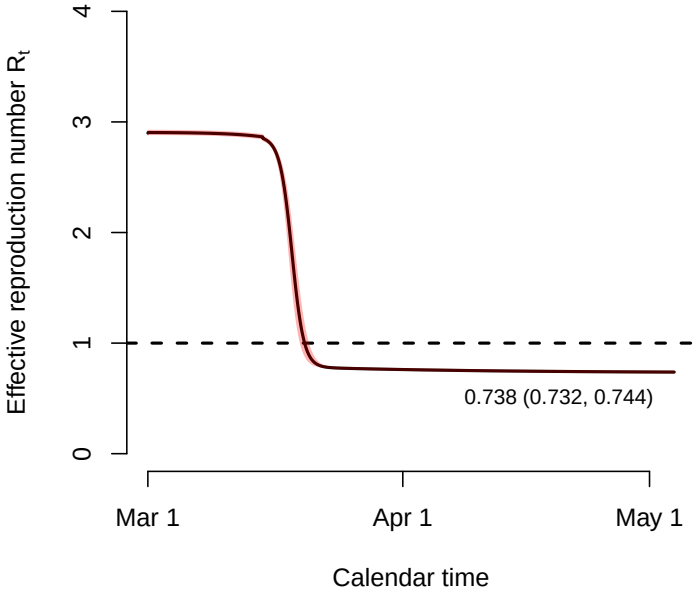

Figure F3: Time-dependent effective reproduction number.

accommodating delay in mortality following infection. According to Molenberghs et al. (2020), the IFRs in the nursing home population are much higher compared to those in the non-nursing

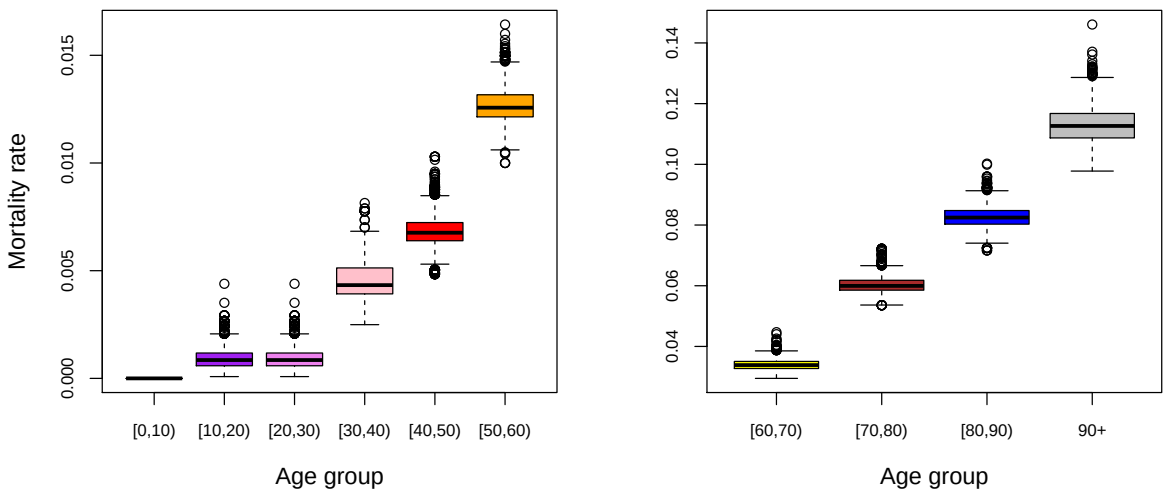

Figure F4: Boxplots of the marginal posterior distributions of the mortality rates by age group.

home population and differences in IFRs in older age categories are linked to frailty and underlying prevalence of comorbidities, characteristics which are very much different in nursing and non-nursing home populations.

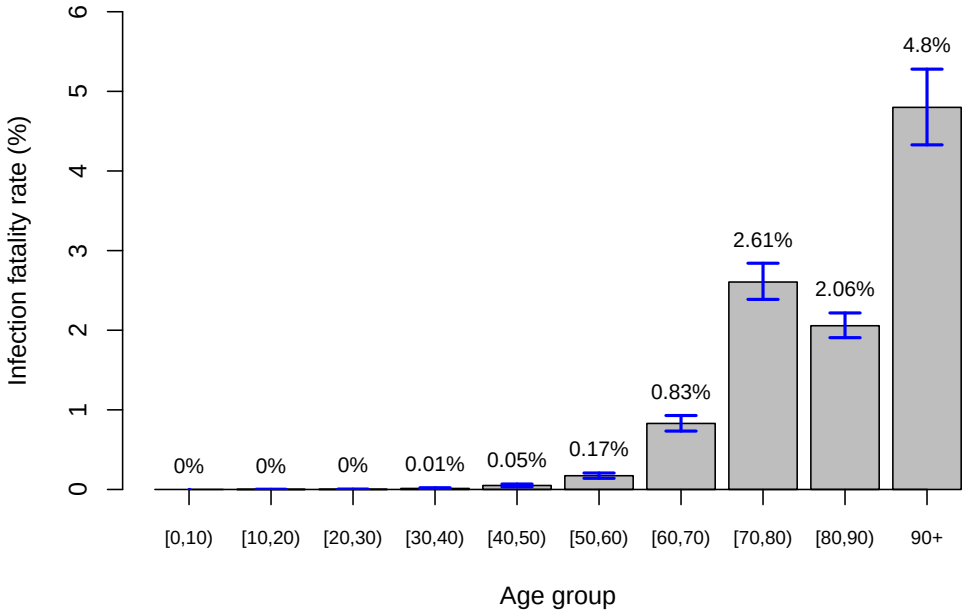

Figure F5: Infection fatality rates by age group with 95% credible intervals in blue.

F.7 Cumulative number of hospitalizations (exit scenario analyses)

In Figure F6, we show the total number of hospitalizations over time in the different scenarios S7–S12. In general, the cumulative number of hospitalizations is highest in scenarios S10–S12 with the cumulative number of hospitalizations on average being comparable by the end of December, 2020 in scenarios S7–S9 on the one hand, and S10–S12 on the other hand.

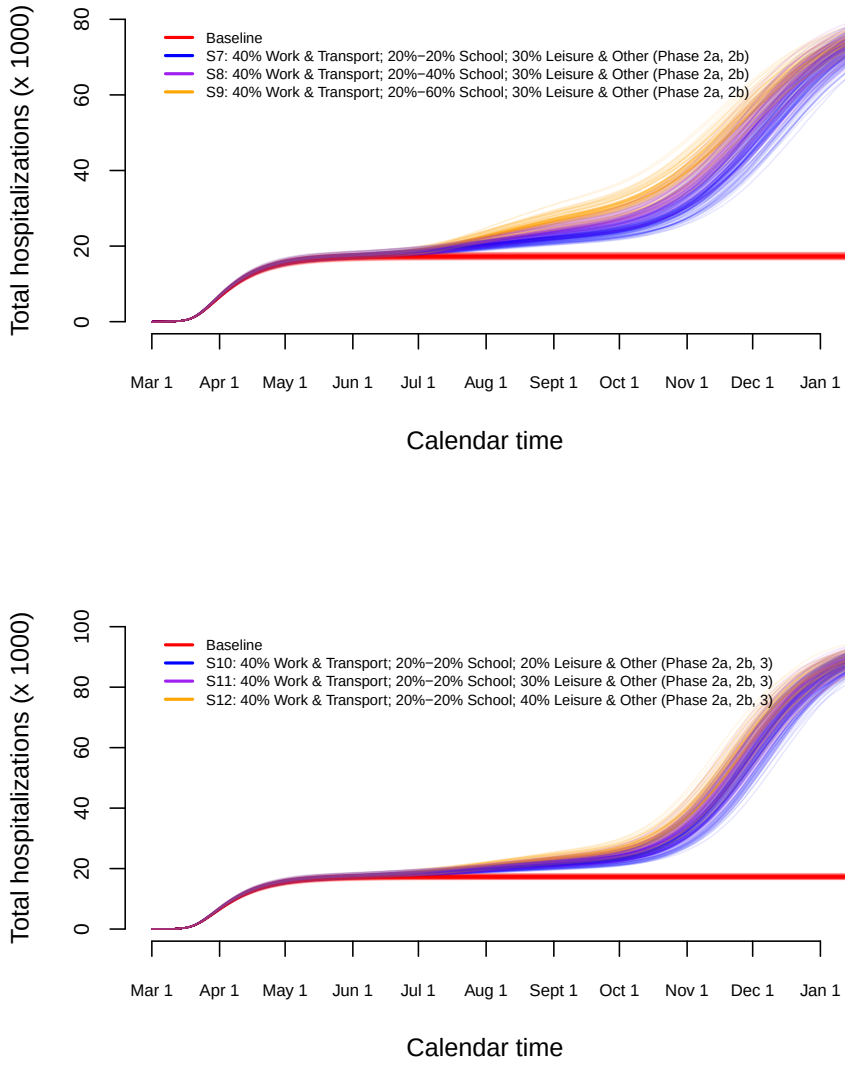

Figure F6: Long-term predictions of the impact of various exit strategies on the total number of hospitalizations over time.

F.8 Sensitivity to transmission potential of children

As a sensitivity analysis, we studied the impact of varying the infectiousness of children on the final results. As mentioned in Section B.2, the role of children is still unclear albeit that some authors have tried to investigate the transmission potential of children. More specifically, children present a smaller viral load upon contracting the infection [1, 2, 3, 41, 42]. Furthermore, some authors claim

that children have a reduced transmissibility [43, 44], albeit that it remains unclear whether this is due to a lower probability of presenting symptoms and differential transmissibility for asymptomatic versus symptomatic cases or directly by lowering infectiousness for both asymptomatic and symptomatic children.

We present stochastic simulation results based on a 50% reduction in the infectiousness of symptomatic and asymptomatic children in age category $[0, 10)$. Posterior measures are very similar with only a small increase in the basic reproduction number R_0 (3.021, 95% credible interval: 2.987, 3.056).

In Figures F7 and F8, we depict similar exit scenarios as the long-term scenarios S7–S12 presented in the main text. In general, the reduction in infectiousness leads to a decrease in peak size of the next wave of hospitalizations with a small delay in timing of the peak.

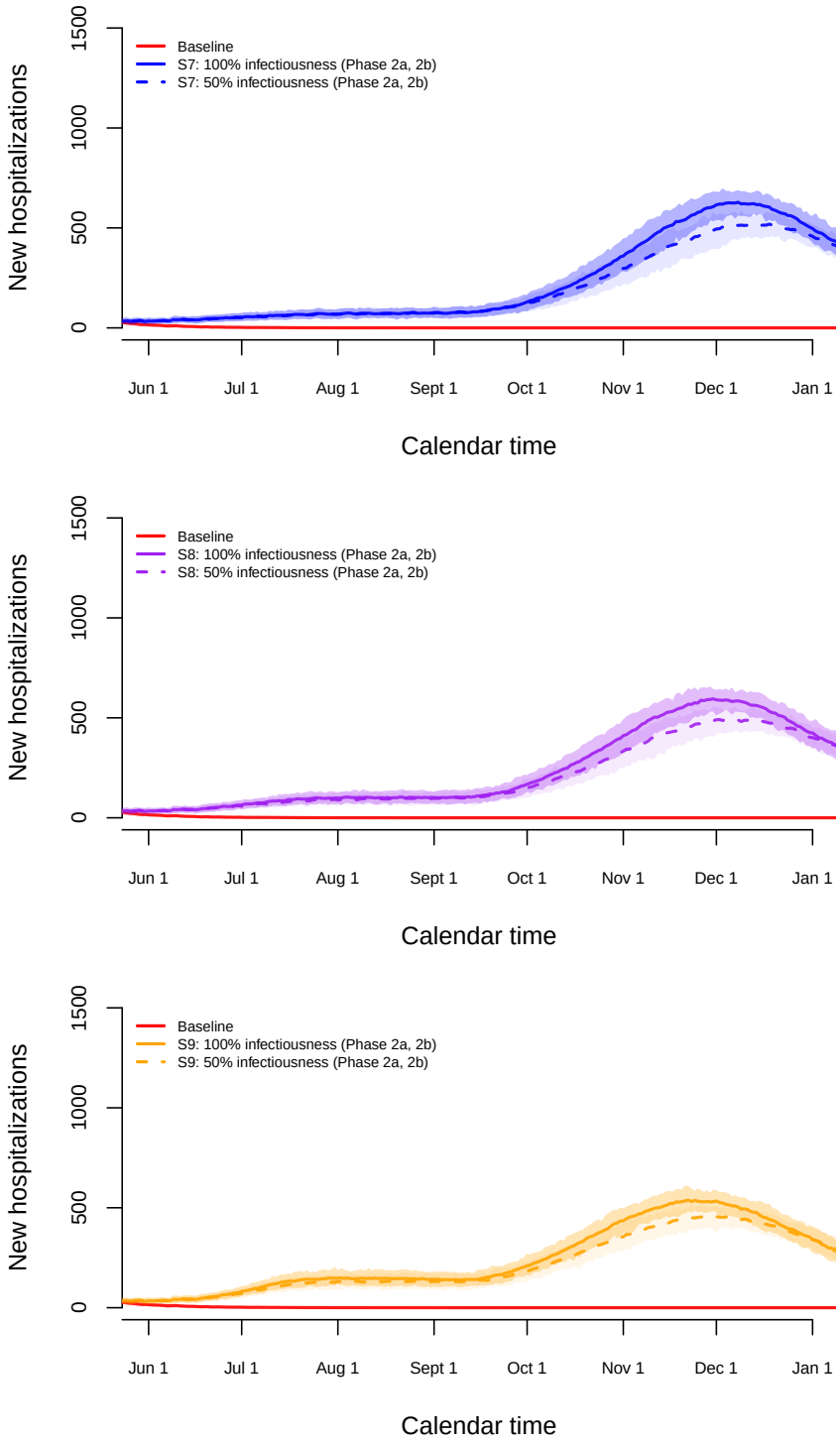

Figure F7: Long-term predictions of the impact of various exit strategies S7–S9 on the number of new hospitalizations.

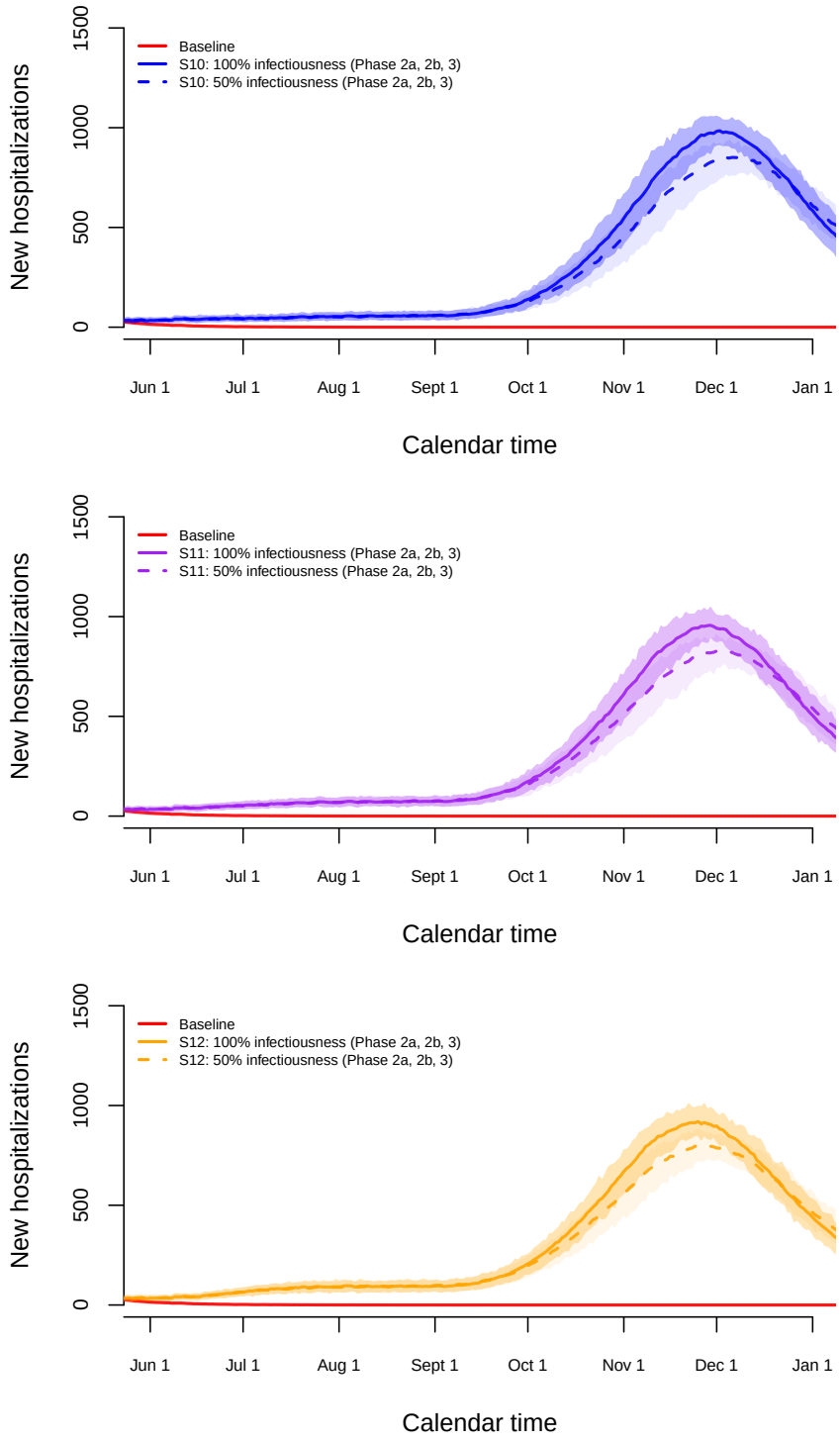

Figure F8: Long-term predictions of the impact of various exit strategies S10–S12 on the number of new hospitalizations.

F.9 Sensitivity to diagnostic performance of serological IgG ELISA test

Changing the underlying sensitivity curve, leaving the presumed impact of intervention measures on the reduction of social contacts unchanged, mainly leads to a decrease in the posterior mean

for R_0 to 2.962 (95% credible interval (CI): 2.909, 3.018) and an increase for ρ^{-1}, the average length of the latent period, with posterior mean 5.101 (95% CI: 5.016, 5.190). In Figure F9, the impact on the estimated overall prevalence over time is depicted. The estimated overall prevalence and corresponding 95% credible interval are shown for the original sensitivity curve (black dashed line with gray shaded area) and the alternative sensitivity curve (red solid line with red shaded area) as presented in Appendix E. In case of the different sensitivity curve the estimated prevalence is lower which is as expected given the faster detectability of IgG antibodies after SARS-CoV-2 infection. The estimated seroprevalence at the cross-sectional time points is almost identical for the two sensitivity curves (not shown).

In addition, we present the IFRs under different assumptions with regard to the sensitivity curve

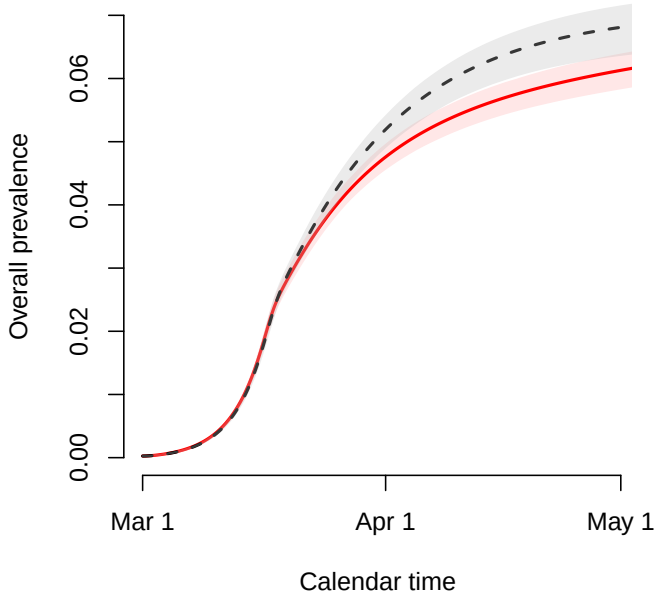

Figure F9: Estimated time-dependent prevalence of COVID-19 under different assumptions for the sensitivity of the IgG ELISA test.

in Figure F10. A small increase in estimated average IFRs is observed for the higher age categories in case of the new sensitivity curve (red line in Figure E2).

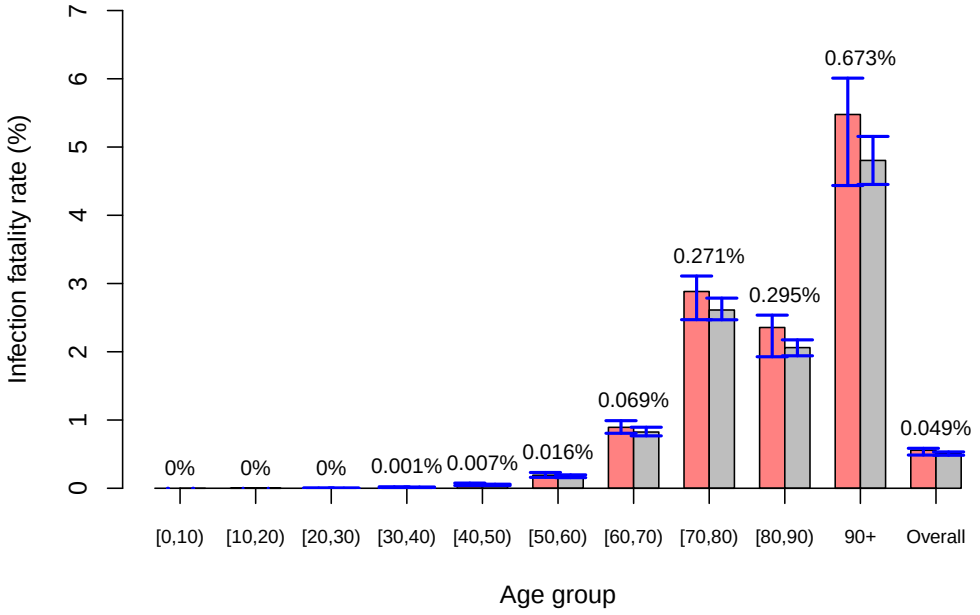

Figure F10: Infection fatality rates by age group with 95% credible intervals in blue and different sensitivity curves for the IgG ELISA test. Differences in mean IFRs between the two analyses indicated on top of the grouped bars per age category.

References

[1] Jones, T.C., Mühlemann, B., Veith, T., Zuchowski, M., Hofmann, J., Stein, A., Edelmann, A., Corman, V.M., Drosten, C.: An analysis of SARS-CoV-2 viral load by patient age. German Research network Zoonotic Infectious Diseases website (2020)

[2] Held, L.: A Discussion and Reanalysis of the Results Reported in Jones et Al. (2020): "An Analysis of SARS-CoV-2 Viral Load by Patient age". https://osf.io/bkuar/

[3] McConway, K., Spiegelhalter, D.: Is SARS-CoV-2 Viral Load Lower in Young Children than Adults? Jones et al Provide Evidence that It Is (in Spite of Their Claims to the Contrary). https://medium.com/@d_spiegel/is-sars-cov-2-viral-load-lower-in-young-children-than-adults-8b4116d28353

[4] Davies, N.G., Klepac, P., Liu, Y., Prem, K., Jit, M., CMMID COVID-19 working group, Eggo, R.M.: Age-dependent effects in the transmission and control of COVID-19 epidemics. Nature Medicine **26**, 1205–1211 (2020). doi:10.1101/2020.03.24.20043018. https://www.medrxiv.org/content/early/2020/05/03/2020.03.24.20043018.full.pdf

[5] Li, Q., Guan, X., Wu, P., Wang, X., Zhou, L., Tong, Y., Ren, R., Leung, K.S.M., Lau, E.H.Y., Wong, J.Y., Xing, X., Xiang, N., Wu, Y., Li, C., Chen, Q., Li, D., Liu, T., Zhao, J., Liu, M., Tu, W., Chen, C., Jin, L., Yang, R., Wang, Q., Zhou, S., Wang, R., Liu, H., Luo, Y., Liu, Y., Shao, G., Li, H., Tao, Z., Yang, Y., Deng, Z., Liu, B., Ma, Z., Zhang, Y., Shi, G., Lam, T.Y.T., Wu, J.T., Gao, G.F., Cowling, B.J., Yang, B., Leung, G.M., Feng, Z.: Early transmission dynamics in Wuhan, China, of novel coronavirus–infected pneumonia. New England Journal of Medicine **382**(13), 1199–1207 (2020). doi:10.1056/NEJMoa2001316. PMID: 31995857. https://doi.org/10.1056/NEJMoa2001316

[6] Wu, J.T., Leung, K., Bushman, M., Kishore, N., Niehus, R., de Salazar, P.M., Cowling, B.J., Lipsitch, M., Leung, G.M.: Estimating clinical severity of COVID-19 from the transmission dynamics in Wuhan, China. Nature Medicine **26**, 506–510 (2020). doi:10.1038/s41591-020-0822-7

[7] CDC COVID-19 Response Team: Severe outcomes among patients with coronavirus disease 2019 (COVID-19) – United States, February 12–March 16, 2020. Technical report, Center for Disease Control (2020)

[8] Riou, J., Hauser, A., Counotte, M., Althaus, C.: Adjusted age-specific case fatality ratio during the COVID-19 epidemic in Hubei, China, January and February 2020. medRxiv (2020). doi:10.1101/2020.03.04.20031104

[9] Lauer, S.A., Grant, K.H., Bi, Q., Jones, F.K., Zheng, Q., Meredith, H.R., Azman, A.S., Reich, N.G., Lessler, J.: The incubation period of 2019-ncov from publicly reported confirmed cases: estimation and application. Annals of Internal Medicine **172**(9), 577–582 (2020). doi:10.1101/2020.02.02.20020016.

[10] Linton, N.M., T., K., Y., Y., Hayashi, K., Akhmetzhanov, A.R., Sung-Mok, J., Baoyin, Y., Kinoshita, R., Nishiura, H.: Incubation period and other epidemiological characteristics of 2019 novel coronavirus infections with right truncation: A statistical analysis of publicly available case data. Journal of Clinical Medicine Research **9**(2), 538 (2020). doi:10.3390/jcm9020538

[11] Guan, W.-j., Ni, Z.-y., Hu, Y., Liang, W.-h., Ou, C.-q., He, J.-x., Liu, L., Shan, H., Lei, C.-l., Hui, D.S.C., Du, B., Li, L.-j., Zeng, G., Yuen, K.-Y., Chen, R.-c., Tang, C.-l., Wang, T., Chen, P.-y., Xiang, J., Li, S.-y., Wang, J.-l., Liang, Z.-j., Peng, Y.-x., Wei, L., Liu, Y., Hu, Y.-h.,

Peng, P., Wang, J.-m., Liu, J.-y., Chen, Z., Li, G., Zheng, Z.-j., Qiu, S.-q., Luo, J., Ye, C.-j., Zhu, S.-y., Zhong, N.-s.: Clinical characteristics of coronavirus disease 2019 in china. New England Journal of Medicine **382**(18), 1708–1720 (2020). doi:10.1056/NEJMoa2002032

[12] Lourenco, J., Paton, R., Ghafari, M., Kraemer, M., Thompson, C., Simmonds, P., Klenerman, P., Gupta, S.: Fundamental principles of epidemic spread highlight the immediate need for large-scale serological surveys to assess the stage of the SARS-CoV-2 epidemic. medRxiv (2020). doi:10.1101/2020.03.24.20042291. https://www.medrxiv.org/content/early/2020/03/26/2020.03.24.20042291.full.pdf

[13] Ma, S., Zhang, J., Zeng, M., Yun, Q., Guo, W., Zheng, Y., Zhao, S., Wang, M.H., Yang, Z.: Epidemiological parameters of coronavirus disease 2019: a pooled analysis of publicly reported individual data of 1155 cases from seven countries. medRxiv (2020). doi:10.1101/2020.03.21.20040329. https://www.medrxiv.org/content/early/2020/03/24/2020.03.21.20040329.full.pdf

[14] Hu, Z., Song, C., Xu, C., Jin, G., Chen, Y., Xu, X., Ma, H., Chen, W., Lin, Y., Zheng, Y., Wang, J., Hu, Z., Yi, Y., Shen, H.: Clinical characteristics of 24 asymptomatic infections with COVID-19 screened among close contacts in Nanjing, China. Science China Life Sciences **63**(5), 706–711 (2020). doi:10.1007/s11427-020-1661-4

[15] Davies, N.G., Kucharski, A.J., Eggo, R.M., Gimma, A., CMMID COVID-19 Working Group, Edmunds, W.J.: Effectsof non-pharmaceutical interventions on COVID-19 cases, deaths and demand for hospital services in the UK: a modelling study. The Lancet Public Health **5**(7), 375–385 (2020). https://www.medrxiv.org/content/early/2020/04/06/2020.04.01.20049908.full.pdf

[16] He, X., Lau, E.H.Y., Wu, P., Deng, X., Wang, J., Hao, X., Lau, Y.C., Wong, J.Y., Guan, Y., Tan, X., Mo, X., Chen, Y., Liao, B., Chen, W., Hu, F., Zhang, Q., Zhong, M., Wu, Y., Zhao, L., Zhang, F., Cowling, B.J., Li, F., Leung, G.M.: Temporal dynamics in viral shedding and transmissibility of COVID-19. Nature Medicine **26**, 672–675 (2020). doi:10.1038/s41591-020-0869-5

[17] Tindale, L., Coombe, M., Stockdale, J.E., Garlock, E., Lau, W.Y.V., Saraswat, M., Lee, Y.-H.B., Zhang, L., Chen, D., Wallinga, J., Colijn, C.: Transmission interval estimates suggest pre-symptomatic spread of COVID-19. medRxiv (2020). doi:10.1101/2020.03.03.20029983. https://www.medrxiv.org/content/early/2020/03/06/2020.03.03.20029983.full.pdf

[18] Faes, C., Abrams, S., Van Beckhoven, D., Meyfroidt, G., Vlieghe, E., Hens, N.: Time between symptom onset, hospitalisation and recovery or death: a statistical analysis of different time-delay distributions in Belgian COVID-19 patients. International Journal of Environmental Research and Public Health **17**(20), 7560 (2020). doi:10.3390/ijerph17207560

[19] Sanche, S., Yen, T.L., Xu, C., Romero-Severson, E., Hengartner, N., Ke, R.: High contagiousness and rapid spread of Severe Acute Respiratory Syndrome coronavirus 2. Emerging infectious diseases **26**(7) (2020). doi:10.3201/eid2607.200282

[20] Nishiura, H., Jung, S.-M., Linton, N.M., Kinoshita, R., Yang, Y., Hayashi, K., Kobayashi, T., Yuan, B., Akhmetzhanov, A.R.: The extent of transmission of novel coronavirus in Wuhan, China, 2020. Journal of Clinical Medicine **9**(2) (2020). doi:10.3390/jcm9020330

[21] Nishiura, H., Kobayashi, T., Yang, Y., Hayashi, K., Miyama, T., Kinoshita, R., Linton, N.M., Jung, S.-M., Yuan, B., Suzuki, A., Akhmetzhanov, A.R.: The rate of underascertainment of novel coronavirus (2019-nCoV) infection: Estimation using Japanese passengers data on evacuation flights. Journal of Clinical Medicine **9**(2) (2020). doi:10.3390/jcm9020419

[22] Mizumoto, K., Kagaya, K., Zarebski, A., Chowell, G.: Estimating the asymptomatic proportion of coronavirus disease 2019 (COVID-19) cases on board the Diamond Princess cruise ship, Yokohama, Japan, 2020. Eurosurveillance **25**(10) (2020). doi:10.2807/1560-7917.ES.2020.25.10.2000180

[23] Chinese Center for Disease Control and Prevention http://www.chinacdc.cn/en

[24] Coronavirus — EpiCentro, Instituto Superiore di Sanità http://www.epicentro.iss.it/coronavirus/

[25] Verity, R., Okell, L.C., Dorigatti, I., Winskill, P., Whittaker, C., Imai, N., Cuomo-Dannenburg, G., Thompson, H., Walker, P.G.T., Fu, H., Dighe, A., Griffin, J.T., Baguelin, M., Bhatia, S., Boonyasiri, A., Cori, A., Cucunubá, Z., FitzJohn, R., Gaythorpe, K., Green, W., Hamlet, A., Hinsley, W., Laydon, D., Nedjati-Gilani, G., Riley, S., van Elsland, S., Volz, E., Wang, H., Wang, Y., Xi, X., Donnelly, C.A., Ghani, A.C., Ferguson N., M.: Estimates of the severity of coronavirus disease 2019: a model-based analysis. The Lancet Infectious Diseases **20**(6), 669–677 (2020)

[26] Zhao, S., Lin, Q., Ran, J., Musa, S.S., Yang, G., Wang, W., Lou, Y., Gao, D., Yang, L., He, D., Wang, M.H.: Preliminary estimation of the basic reproduction number of novel coronavirus 2019-nCoV in China, from 2019 to 2020: A data-driven analysis in the early phase of the outbreak. International Journal of Infectious Diseases **92**, 214–217 (2020). doi:10.1016/j.ijid.2020.01.050

[27] Kucharski, A.J., Russell, T.W., Diamond, C., Liu, Y., Edmunds, J., Funk, S., Eggo, R.M., on behalf of the Centre for Mathematical Modelling of Infectious Diseases COVID-19 working group: Early dynamics of transmission and control of COVID-19: a mathematical modelling study. Lancet Infectious Diseases **20**, 553–558 (2020)

[28] Turk, P.J., Chou, S.-H., Kowalkowski, M.A., Palmer, P.P., Priem, J.S., Spencer, M.D., Taylor, Y.J., McWilliams, A.D.: Modeling COVID-19 latent prevalence to assess a public health intervention at a state and regional scale. JMIR Public Health and Surveillance **6**(2), 19353 (2020). doi:10.2196/19353. https://www.medrxiv.org/content/early/2020/05/20/2020.04.14.20063420.full.pdf

[29] Park, S.W., Cornforth, D.M., Dushoff, J., Weitz, J.S.: The time scale of asymptomatic transmission affects estimates of epidemic potential in the COVID-19 outbreak. Epidemics **31**, 100392 (2020). doi:10.1016/j.epidem.2020.100392

[30] Di Domenico, L., Pullano, G., Sabbatini, C.E., Boëlle, P.-Y., Colizza, V.: Expected impact of lockdown in Île-de-France and possible exit strategies. BMC Medicine **18**(240) (2020)

[31] Tang, B., Xia, F., Bragazzi, N.L., Wang, X., He, S., Sun, X., Tang, S., Xiao, Y., Wu, J.: Lessons drawn from China and South Korea for managing COVID-19 epidemic: insights from a comparative modeling study. medRxiv (2020). doi:10.1101/2020.03.09.20033464. https://www.medrxiv.org/content/early/2020/03/13/2020.03.09.20033464.full.pdf

[32] Cereda, D., Tirani, M., Rovida, F., Demicheli, V., Ajelli, M., Poletti, P., Trentini, F., Guzzetta, G., Marziano, V., Barone, A., Magoni, M., Deandrea, S., Diurno, G., Lombardo, M., Faccini, M., Pan, A., Bruno, R., Pariani, E., Grasselli, G., Piatti, A., Gramegna, M., Baldanti, F., Melegaro, A., Merler, S.: The early phase of the COVID-19 outbreak in Lombardy, Italy. arXiv (2020). 2003.09320

[33] Gatto, M., Bertuzzo, E., Mari, L., Miccoli, S., Carraro, L., Casagrandi, R., Rinaldo, A.: Spread and dynamics of the COVID-19 epidemic in Italy: Effects of emergency containment measures. Proceedings of the National Academy of Sciences **117**(19), 10484–10491 (2020)

[34] Muniz-Rodriguez, K., Fung, I.C.-H., Ferdosi, S.R., Ofori, S.K., Lee, Y., Tariq, A., Chowell, G.: Transmission potential of COVID-19 in Iran. medRxiv (2020). doi:10.1101/2020.03.08.20030643. https://www.medrxiv.org/content/early/2020/04/14/2020.03.08.20030643.full.pdf

[35] Van Kerckhove, K., Hens, N., Edmunds, W.J., Eames, K.T.D.: The impact of illness on social networks: implications for transmission and control of influenza. American Journal of Epidemiology **178**(11), 1655–1662 (2013). doi:10.1093/aje/kwt196

[36] Spiegelhalter, D.J., Best, N.G., Carlin, B.P., Van Der Linde, A.: Bayesian measures of model complexity and fit. Journal of the Royal Statistical Society, Series B **64**(4), 583–639 (2002)

[37] Herzog, S., De Bie, J., Abrams, S., Wouters, I., Ekinci, E., Patteet, L., Coppens, A., De Spiegeleer, S., Beutels, P., Van Damme, P., Hens, N., Theeten, H.: Seroprevalence of IgG antibodies against SARS coronavirus 2 in Belgium - a serial prospective cross-sectional nationwide study of residual samples. medRxiv (2020)

[38] Lou, B., Li, T., Zheng, S., Su, Y., Li, Z., Liu, W., Yu, F., Ge, S., Zou, Q., Yuan, Q., Lin, S., Hong, C., Yao, X., Zhang, X., Wu, D., Zhou, G., Hou, W., Li, T., Zhang, Y., Zhang, S., Fan, J., Zhang, J., Xia, N., Chen, Y.: Serology characteristics of SARS-CoV-2 infection since the exposure and post symptoms onset. European Respiratory Journal **57**(2) (2020). doi:10.1183/13993003.00763-2020. https://www.medrxiv.org/content/early/2020/03/27/2020.03.23.20041707.full.pdf

[39] Borremans, B., Gamble, A., Prager, K.C., Helman, S.K., McClain, A.M., Cox, C., Savage, V., Lloyd-Smith, J.O.: Quantifying antibody kinetics and RNA detection during early-phase SARS-CoV-2 infection by time since symptom onset. Elife **9**, 60122 (2020). doi:10.7554/eLife.60122

[40] Molenberghs, G., Faes, C., Verbeeck, J., Deboosere, P., Abrams, S., Willem, L., Aerts, J., Theeten, H., De Vleesschauwer, B., Bustos Sierra, N., Renard, F., Herzog, S., Lusyne, P., Van der Heyden, J., Van Oyen, H., Van Damme, P., Hens, N.: Belgian COVID-19 mortality, excess deaths, number of deaths per million, and infection fatality rates (8 march – 28 june, 2020). medRxiv (2020)

[41] Stoye, J.: A critical assessment of some recent work on COVID-19. ArXiv, 2005–10237 (2020)

[42] Curtis, D.: Children have lower SARS-CoV-2 viral load than adults. Preprints (2020). doi:10.20944/preprints202005.0367.v1

[43] Boast, A., Munro, A., Goldstein, H.: An evidence summary of paediatric COVID-19 literature. Don't Forget the Bubbles (2020). doi:10.31440/DFTB.24063

[44] Heavey, L., Casey, G., Kelly, C., Kelly, D., McDarby, G.: No evidence of secondary transmission of COVID-19 from children attending school in Ireland, 2020. Eurosurveillance **25**(21) (2020). doi:10.2807/1560-7917.ES.2020.25.21.2000903